

# Multifunctional brushes made from carbon nanotubes

ANYUAN CAO<sup>1</sup>, VINOD P. VEEDU<sup>2</sup>, XUESONG LI<sup>1</sup>, ZHAOLING YAO<sup>1</sup>, MEHRDAD N. GHASEMI-NEJHAD<sup>2</sup> AND PULICKEL M. AJAYAN<sup>1\*</sup>

<sup>1</sup>Department of Materials Science & Engineering, Rensselaer Polytechnic Institute, Troy, New York 12180, USA

<sup>2</sup>Department of Mechanical Engineering, University of Hawaii at Manoa, Honolulu, Hawaii 96822, USA

\*e-mail: ajayan@rpi.edu

Published online: 12 June 2005; doi:10.1038/nmat1415

**B**rushes are common tools for use in industry and our daily life, performing a variety of tasks such as cleaning, scraping, applying and electrical contacts. Typical materials for constructing brush bristles include animal hairs, synthetic polymer fibres and metal wires (see, for example, ref. 1). The performance of these bristles has been limited by the oxidation and degradation of metal wires, poor strength of natural hairs, and low thermal stability of synthetic fibres. Carbon nanotubes<sup>2,3</sup>, having a typical one-dimensional nanostructure, have excellent mechanical properties, such as high modulus and strength<sup>4–6</sup>, high elasticity and resilience<sup>7</sup>, thermal conductivity<sup>8</sup> and large surface area (50–200 m<sup>2</sup> g<sup>-1</sup>)<sup>9</sup>. Here we construct multifunctional, conductive brushes with carbon nanotube bristles grafted on fibre handles, and demonstrate their several unique tasks such as cleaning of nanoparticles from narrow spaces, coating of the inside of holes, selective chemical adsorption, and as movable electromechanical brush contacts and switches. The nanotube bristles can also be chemically functionalized for selective removal of heavy metal ions.

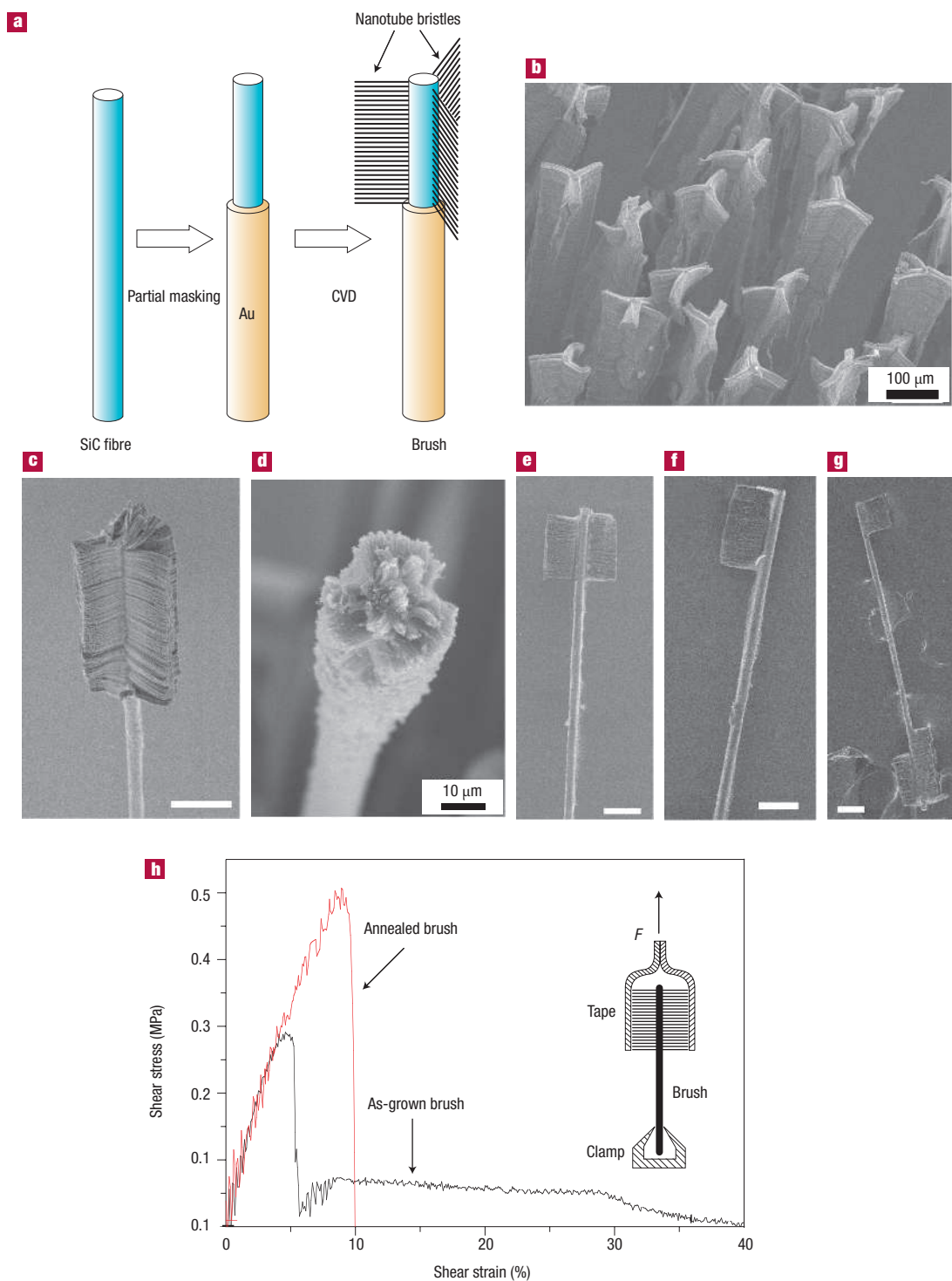
The nanotube brush consists of a silicon carbide fibre (SiC, diameter 16 µm) as the handle and aligned multiwalled carbon nanotubes grafted on the fibre ends as bristles. The nanotubes (average diameter 30 nm) were grown by selective chemical vapour deposition (CVD) with ferrocene and xylene as the precursors<sup>10,11</sup>. Before CVD, individual SiC fibres were partially masked by a 15-nm Au layer except for the top ends (Fig. 1a) and placed vertically in the furnace (Supplementary Information, Fig. S1a). The Au layer serves as a physical mask<sup>12</sup> to limit the growth of the nanotubes to the unmasked fibre ends. Figure 1b shows the scanning electron microscope (SEM, JEOL JSM-6330-F) image of the top morphology of as-grown nanotubes on fibres. Here, the nanotubes grew in three prongs symmetrically distributed around the centre fibre, and have a uniform length (~60 µm after 40 minutes' growth) along the fibre axis. Within the prongs, nanotubes are well aligned with tips exposed at the edges (Supplementary Information, Fig. S1).

Figure 1c shows an individual brush with 60-µm-long nanotube bristles spanning over 300 µm. Compared with current commercial brushes having bristles of 0.038–1.9 mm in diameter and a core block size of more than 3 mm, these nanotube brushes have bristle sizes 1,000 times smaller and the overall size is decreased more than

20 times. The total weight of a single brush (plus a 1-cm-long fibre handle) is less than 50 µg. Nonetheless, the brush as shown in Fig. 1c contains nearly  $1.7 \times 10^6$  bristles (nanotubes), with an area density of  $\sim 1.2 \times 10^8$  mm<sup>-2</sup> (calculation based on the measurements of sample weight, see Methods), five orders higher than available commercial brushes ( $\sim 10^3$  mm<sup>-2</sup>). When these nanotube bristles are placed on a plain surface (here we assume that all the nanotubes have the same height), the contact area (where the nanotube tips touch the surface) is  $1.27 \times 10^3$  µm<sup>2</sup>, about 8.8% of the total bristle front surface ( $14.4 \times 10^3$  µm<sup>2</sup>), slightly higher than a conventional toothbrush having a contact area of 7.9% (based on a head size of  $1 \times 2$  cm<sup>2</sup> and 500 bristles 0.2 mm in diameter, 1 cm in height). The actual contact area could be larger if the bristles are pressed against the contacting surface and nanotubes are bent (as larger portions of the nanotubes would engage the surface). In addition, once immersed in a solution, the total liquid–nanotube contact area is  $9.8 \times 10^6$  µm<sup>2</sup> over a bristle volume of  $8.64 \times 10^5$  µm<sup>3</sup>. The contact surface area per volume is about  $11.3$  µm<sup>2</sup> µm<sup>-3</sup>, three orders higher than a typical toothbrush ( $1.57 \times 10^{-2}$  µm<sup>2</sup> µm<sup>-3</sup>).

Various styles of brushes were obtained by designing the Au mask area on SiC fibres and growth conditions. The brush size, including trim length (nanotube length) and bristle span (the length of handle covered by bristles), were well controlled during the CVD process. The trim length can be varied from hundreds down to a few micrometres depending on the growth time. By adjusting the Au-masked portion of SiC fibre, we have obtained brushes with bristle spans ranging from several micrometres to millimetres. For example, Fig. 1d shows a brush with 30-µm span and 10-µm trim length formed from nanotubes grown for a short time (~5 minutes). The geometry of the bristles can also be made different, such as three prongs like a dust-sweeper (Fig. 1c), two prongs resembling a hand-held fan (Fig. 1e), and a one-prong toothbrush (Fig. 1f; see Methods). Also, Fig. 1g shows a double-ended brush (with different bristle geometries and spans on each end) prepared by masking gold on the middle portion of the fibre. Brushes having multiple bristles, regularly distributed along the handle, were fabricated by patterning gold mask along the fibre (Supplementary Information, Fig. S2).

As the nanotubes are rooted on the surface of SiC fibres by direct growth, it is necessary to characterize the adhesion between



**Figure 1** Nanotube brushes of various designs, and the result of mechanical testing from an individual brush structure. **a**, Illustration of partial masking of SiC fibres in order to grow nanotubes only on the fibre top. **b–g**, SEM images. **b**, As-grown nanotubes on top of SiC fibres, forming three prongs symmetrically distributed around each fibre. **c**, A single brush (resembling a dust sweeper) consisting of nanotube bristles and a fibre handle. The bristles have a height (nanotube length) of 60  $\mu\text{m}$ , and span of over 300  $\mu\text{m}$  along the handle. **d**, A smaller brush, with a bristle height of only 10  $\mu\text{m}$  and span of 30  $\mu\text{m}$ . **e**, A two-prong brush resembling a hand-held fan. **f**, A one-prong toothbrush. **g**, A double-ended brush with different bristles on each end. Scale bars in **c**, **e**, **f**, **g**: 50  $\mu\text{m}$ . **h**, Tensile testing of brushes (shear-stress versus strain) for measuring the adhesion strength of nanotube bristles, for both as-grown (black) and annealed (red) brushes. Inset: Illustration of the setup for pulling nanotubes away from the handle.

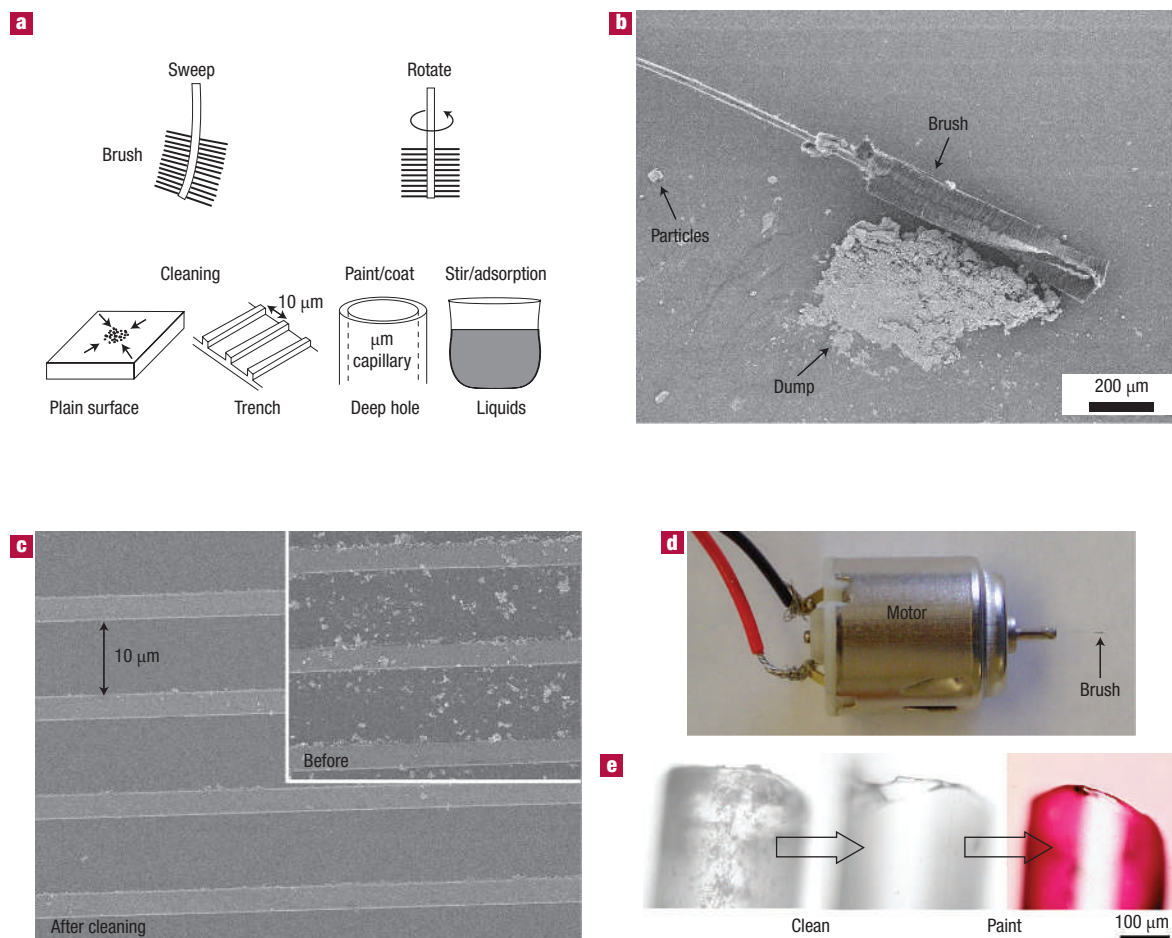


**Figure 2** Multiple functions performed by nanotube brushes. **a**, Schematic illustration of a 'sweep' and 'rotate' brush that can be used to clean nanoparticles and narrow trenches, paint the inside of capillaries, and adsorb liquid chemicals trapped in small area. **b**, A dump of nanoparticles formed by a sweep brush. **c**, 10- $\mu\text{m}$ -wide trenches cleaned by sweeping the brush over the surface. Inset: Dispersed nanoparticles inside trenches before brushing. **d**, A rotate brush attached to an electrical motor. **e**, Use of a rotate brush first to clean the inside of a contaminated capillary (inner diameter of 300  $\mu\text{m}$ ), and then paint the inner wall red.

nanotubes and the fibre for evaluating the brush lifetime. We performed a tensile test to measure this adhesion by mechanically pulling away nanotubes from the handle (see Methods). Here, the nanotubes experienced a shear stress at the nanotube–SiC interface, which eventually strips their ends away from the SiC fibre. The stress–strain curve of an as-grown brush (Fig. 1h) shows a maximum stress of 0.28 MPa before the bristles detached from the handle (for ten brushes tested, this stress ranged over 0.1–0.3 MPa). The adhesion strength can be improved by a subsequent annealing at 950 °C for several hours in argon (the failure stress nearly doubles, see red curve in Fig. 1h). Here the annealing strengthens the interaction between carbon and the underlying silicon (SiC bonding)<sup>13</sup>, thereby substantially enhancing the bristle–handle adhesion. We have performed extensive contact-brush operations (described later) to evaluate the brush lifetimes; for example, the rotating brush, contacting a metal surface in every rotation, after over 0.1 million cycles remains robust without shedding the nanotube bristles. We believe the flexibility of nanotubes can relieve the contact stresses as the brush touches a solid surface on each cycle.

The nanotube brushes integrate a number of useful functions, among which cleaning, painting, adsorption, electrical contact and switching are described here. Two basic brushing actions, 'sweep' and 'rotate', were easily performed for different functions, as illustrated in

Fig. 2a. Sweeping the brush is used for 'dry' cleaning surfaces, for example, removing debris (left behind by processes such as chemical mechanical polishing<sup>14</sup>) or nanoparticles, which is imperative as there has been increasing concern about the health risk caused by the release of nanomaterials<sup>15</sup>. We firstly dispersed nanoparticles (commercial  $\text{Fe}_2\text{O}_3$ , average diameter <50 nm) on a plain silicon wafer, and then swept these particles (and aggregates) into a dump (Fig. 2b) with the brush. The sweeping action was done manually by attaching the fibre to a 5-cm-long quartz rod as an extension handle, and the brush was directed to the nanoparticles under observation with an optical microscope. Although the nanoparticles were moved by the brushes, they didn't stick to the bristles and could be recollected. The same action using a commercial brush (for example, Anchor Set hand-held brush, bristle diameter 0.1 mm, Gordon Brush), left most of the particles untouched. The nanotube brushes were used to clean rough surfaces, for example, narrow trenches (10  $\mu\text{m}$  wide and 100 nm deep, shown in Fig. 2c). This was done by sweeping along the trench direction three or four times, which removed nearly all of the nanoparticles sitting on top of the pattern as well as at the bottom of trenches, indicating that the flexible nanotube bristles can adapt to the geometry of narrow spaces. Sweeping bare SiC fibres only removed some of nanoparticles on the pattern top, but did not accomplish cleaning inside trenches.

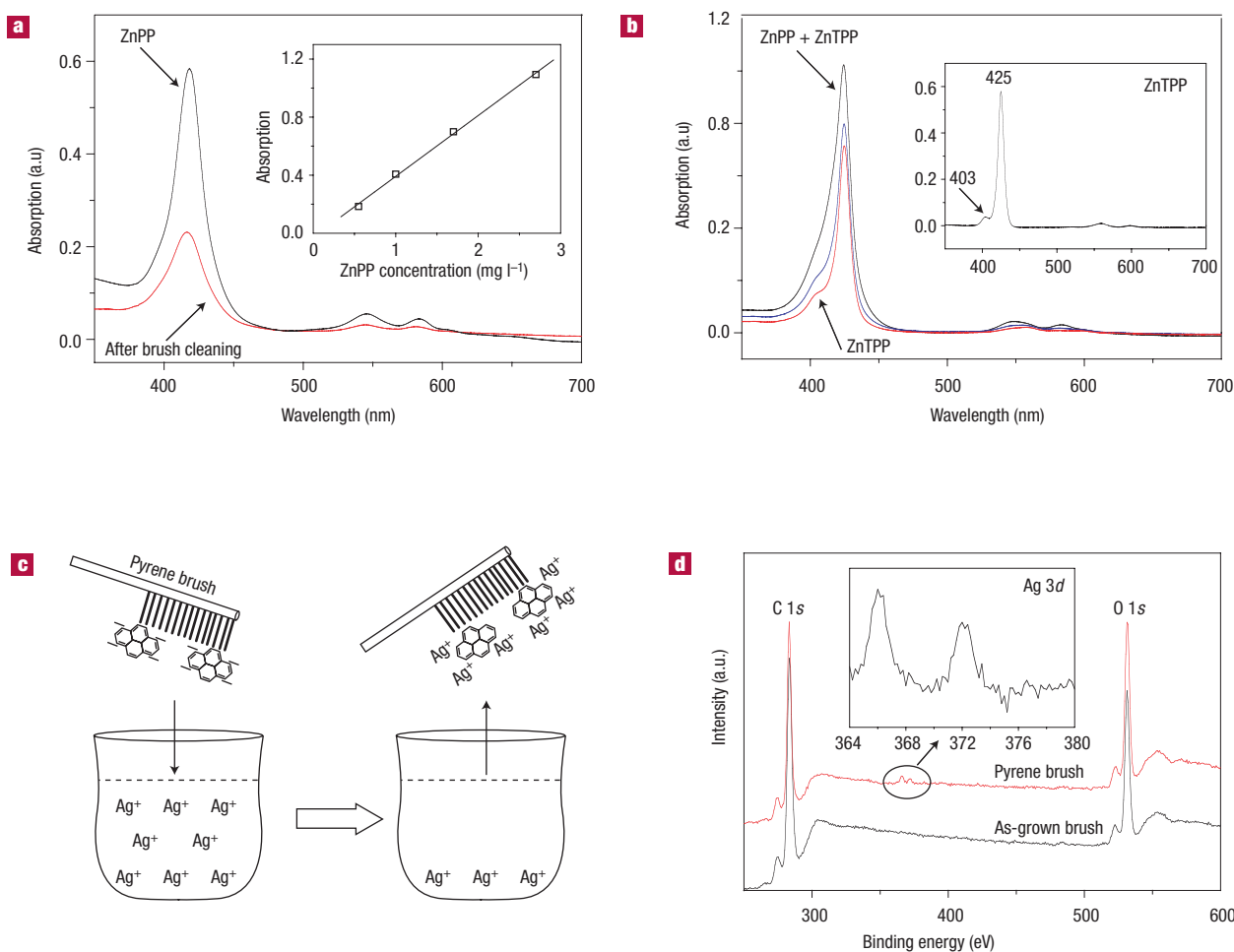


**Figure 3** Selective adsorption of chemicals from solution by nanotube brushes. **a**, Ultraviolet–visible spectrum of ZnPP solution (in DMF) before and after rotate-brushing. The peak at 420 nm is the Soret band of ZnPP. Inset: Characterized ZnPP concentration versus Soret band intensity. The instrument used was an ultraviolet–visible spectrometer (Perkin Elmer, Lambda 2). **b**, Selective adsorption of ZnPP from a mixture of ZnPP (1.35 mg l<sup>-1</sup>) and ZnTPP (0.5 mg l<sup>-1</sup>) after brushing the solution for different times (blue: 2 min; red: 5 min). The emergence of a shoulder (403 nm) near the Soret band (424 nm) indicates more ZnTPP left in the solution whereas ZnPP has been selectively adsorbed. Inset: Ultraviolet–visible absorption spectrum of pure ZnTPP with a characteristic peak at 403 nm (see arrow). **c**, Illustration showing the dipping of a pyrene-functionalized nanotube brush to pick up silver ions in solution. **d**, XPS spectrum of Ag adsorption by as-grown (black) and pyrene-functionalized (red) brushes. Inset: Ag 3d peaks from pyrene-brushes.

We made an electrically driven brush by fixing it on the rotating head of a motor (Fig. 2d), for the purpose of working inside deep holes and capillaries as illustrated in Fig. 2a. For example, a three-prong brush was rotated to sequentially clean and paint the inner wall of a capillary (diameter 300  $\mu\text{m}$ , with pre-dispersed  $\text{Fe}_2\text{O}_3$  nanoparticles), at 2,000 r.p.m. for 5 s. Then the brush was dipped into red paint (gloss enamel, Testors) and then rotated in the capillary again for 5 s, resulting in a uniform red coating on the inner wall (Fig. 2e). Brush-coating has wide applications in thin-film coating and device decoration, and here the brushes may be used as disposables.

A rotating brush is suitable for working in liquid, for example, selective adsorption and removal of organic chemicals (for example, porphyrins, functional dyes for developing photosynthetic materials<sup>16</sup>). In porphyrins, zinc protoporphyrin IX (ZnPP) has a planar molecule (structures in Supplementary Information, Fig. S3), and can adsorb strongly on nanotube surfaces through  $\pi$ - $\pi$  stacking interactions<sup>17</sup>, whereas zinc tetraphenylporphyrin (ZnTPP) is non-planar, only weakly interacting with nanotubes. A nanotube brush was immersed into a solution of ZnPP dissolved in dimethylformamide

(DMF) housed in a capillary and stirred for 4 min at 2,000 r.p.m. Figure 3a shows the ultraviolet–visible absorption spectrum of the solution before and after brush stirring. The ZnPP concentration dropped from 1.5 to 0.6 mg l<sup>-1</sup>, as indicated by the intensity change of the Soret band at 420 nm. Here the porous nanotube bristles act as a ‘molecule sponge’, and suck ZnPP molecules into the channels between nanotubes. Selective adsorption was done by brushing a mixed solution of ZnPP and ZnTPP in DMF for 5 min (Fig. 3b). Although the intensity of the Soret band (at 425 nm) gradually decreased from 1.1 to 0.7, a shoulder at 403 nm clearly emerged, which is a characteristic peak of ZnTPP, indicating that ZnPP has been selectively removed (the concentration of ZnTPP remained unchanged, whereas the relative concentration ratio of ZnPP/ZnTPP decreased from 2.7:1 to 1.1:1). After rotation in solution, the brushes retained their structure and no nanotubes shed and contaminated the solution (Supplementary Information, Fig. S4).

We also functionalized nanotube brushes to remove dissolved species such as heavy metal ions (for example,  $\text{Ag}^+$ ) in solution (for example, silver nitrate, lethal in concentrations of 0.076 g ml<sup>-1</sup>). Ionic

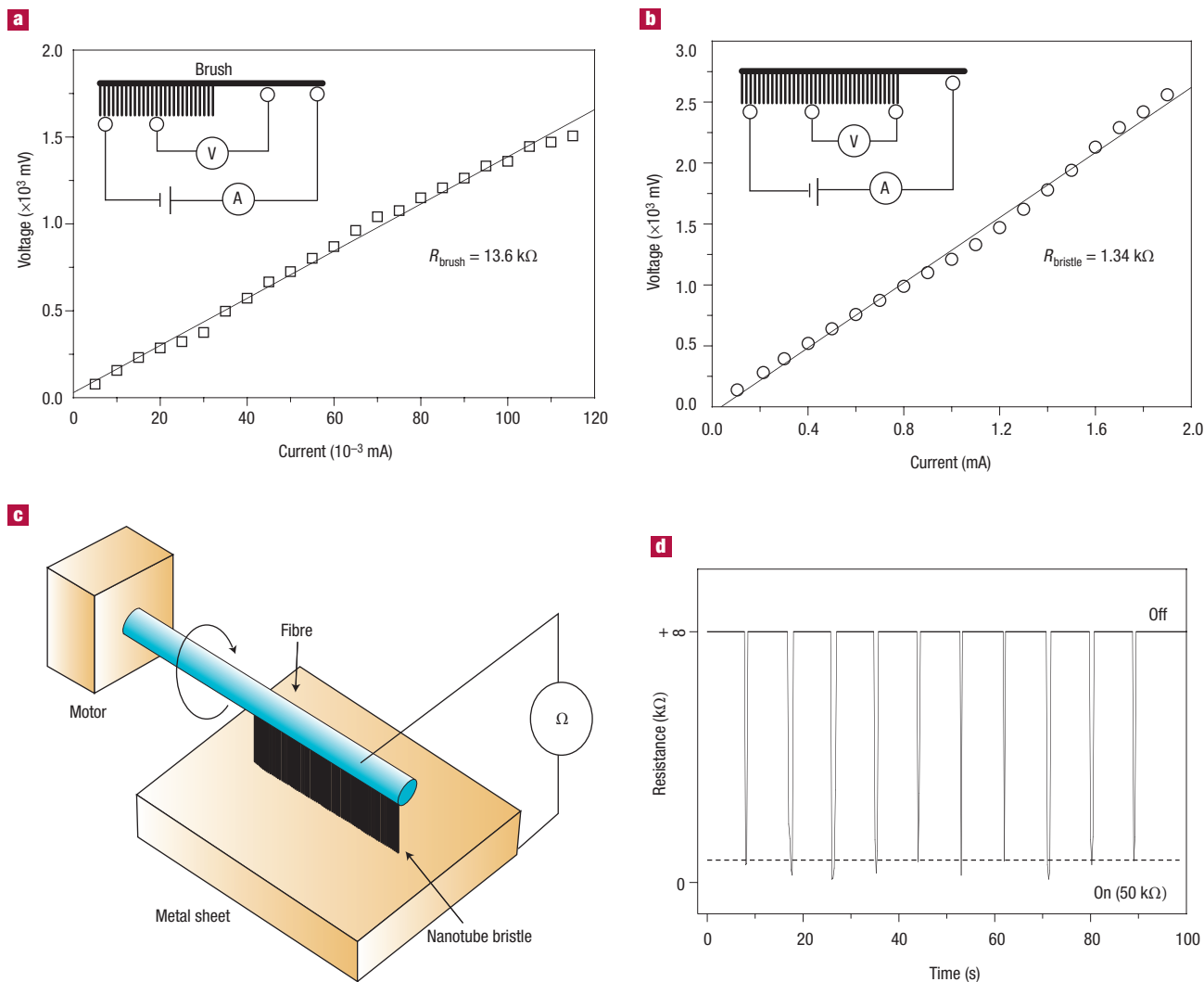


**Figure 4** Electrical characterization of nanotube brushes and the construction of a flexible electromechanical switch. **a**, Four-probe current–voltage measurement of a single brush (1-mm bristle span with 1-mm handle), showing an electrical resistance of  $<15$  k $\Omega$ . **b**, Current–voltage plot of nanotube bristles only, with a resistance of  $<2$  k $\Omega$ . **c**, Design of an electrical switch device based on a motor-driven brush with the nanotube bristles as the touch-contact structure. An ohm meter was connected to the nanotubes and the underlying metal sheet to record the device resistance. **d**, Periodic resistance change while the brush was rotating at a constant speed ( $\sim 7$  r.p.m.), with an exchange of the ‘on’ ( $\sim 50$  k $\Omega$ ) and ‘off’ (infinite) status of the device.

pyrene derivative (1,3,6,8-pyrenetetrasulfonate acid tetrasodium) with three  $\text{SO}_3^-$  per molecule (Supplementary Information, Figs S5 and S6) was grafted onto nanotube brushes to pick up  $\text{Ag}^+$  by the attraction between  $\text{SO}_3^-$  and  $\text{Ag}^+$  through a simple ‘dip’ action (Fig. 3c). The brushes were soaked into 20 ml silver nitrate ( $\text{AgNO}_3$ , 0.1 N) for 10 minutes, which was kept stirred, and then rinsed in distilled water to remove the residue solution on the brush surface. As-grown brushes without any functionalization were tested for reference. The adsorption of silver on brushes was characterized by X-ray photoelectron spectroscopy (XPS) (Perkin Elmer XPS 5500, Mg source). The pyrene brushes show two clear peaks (Ag 3d) at the binding energy of around 370 eV, whereas as-grown brushes do not show observable Ag adsorption (Fig. 3d). Calculation based on the peak (intensity) area of Ag relative to C (done by the RBD AugerScan Software upgrade) shows an Ag percentage of 0.1% (number of atoms). Small particles and aggregates were observed on the brush surface after  $\text{H}_2$  reduction (Supplementary Information, Fig. S7), confirming the adsorption of silver ions.

Finally, as the nanotube bristles are electrically conductive, the brushes could act as flexible/movable contacts. Conductive brushes are commonly used in conjunction with slip rings or commutators to maintain an electrical connection in rotary and linear sliding contact applications<sup>18</sup>. Conventional metal-to-metal contacts have suffered from local welding and formation of insulating interfacial films due to oxidation. The nanotube brushes provide a high level of contact redundancy, and could be miniaturized for coupling in MEMS devices. The total electrical resistance of a 2-mm-long brush ( $R_{\text{brush}}$ ) consisting of 1-mm bristles and a 1-mm handle was measured to be  $\sim 13.6$  k $\Omega$  (Fig. 4a) through a four-probe setup (see Methods), which combines both the contribution from the nanotubes and gold-coated fibre. The resistance from a 2-mm-span nanotube bristles prong ( $R_{\text{bristle}}$ ) was 1.34 k $\Omega$  (Fig. 4b), thus most of the brush resistance (90%) comes from the poorly conducting handle (which can be replaced by a more conducting handle). The resistivity ( $\rho$ ) of pure nanotube bristles is  $\rho = R_{\text{bristle}}S/L = 7.5 \times 10^{-2}$   $\Omega\text{cm}$ , where  $S$  is

the cross-sectional area of a prong of bristle ( $S = 1.12 \times 10^{-3} \text{ mm}^2$  for a prong width and height of 16 and 70  $\mu\text{m}$ , respectively) and  $L$  is the bristle span (2 mm). The nanotube resistivity ( $7.5 \times 10^{-2} \Omega\text{cm}$ ) is similar to previous reports on aligned nanotube films ( $6.6 \times 10^{-2} \Omega\text{cm}$ )<sup>19</sup>. The nanotube bristles are mechanically and electrically stable when being pressed (>300 kPa) or heated to 673 K (Supplementary Information, Fig. S8).

In addition to the role of an electrical contact, the nanotube brushes can act as electromechanical switches. Figure 4c shows a single-prong brush on top of a flat metal pad (as contact electrode), with its fibre handle as a rotating spindle. This configuration can work as a current switch with controllable frequency, determined by the rotating speed of the brush. The 'on' and 'off' state is defined when the nanotubes touch (on) or leave (off) the underlying metal pad during rotation. The oscillation in the resistance changes as the brush rotates is shown in Fig. 4d. An average resistance of  $\sim 50 \text{ k}\Omega$  was seen periodically in every rotation occurring at a constant speed of 7 r.p.m. Much of this resistance is due to the interface between nanotubes and the metal. The switch-on resistance was maintained over several thousand cycles.

The nanotube brushes described here integrate several unique applications, including cleaning of nanoparticles on planar/rough surfaces, painting inside capillary, adsorption of organic solvents and removal of metal ions, and as rotating electrical contacts. These durable, nanotube brushes could serve as versatile, anti-static, heat-tolerant tools in many industrial and environmental applications.

## METHODS

### GROWTH OF NANOTUBES BY CVD

In the CVD process, a solution made by dissolving 0.3 g ferrocene into 30 ml xylene was injected into the furnace through a rotating syringe pump at a constant speed (0.5 ml min<sup>-1</sup>). Argon was flowed at 40 s.c.c.m. to carry the solution into a pre-heated steel bottle (180 °C) before entering the furnace. SiC fibres were put (either vertically or horizontally) in the middle of the furnace. The typical reaction temperature was 800 °C, and the growth time took 10 minutes to one hour. Vertical placement of fibres (as illustrated in Supplementary Information, Fig. S1a) usually yields three nanotube prongs surrounding the fibre. The formation of three-pronged morphology is due to the self-selected growth of dense nanotube arrays as they grow outwards from the cylindrical surface of the fibre, having circular cross-section, as the circumference surrounding the nanotube front surface is enlarged as the front moves away from the fibre nanotube interface. Two- and one-prong structures were obtained by lying the fibres down on a flat surface during CVD, to block the nanotube growth from the unwanted direction.

### GOLD MASKING ON SiC FIBRES

Shadow masking of gold on the SiC fibres were done in a 50-mtorr Ar plasma at an anode voltage of  $\sim 12 \text{ V}$  and a constant current of 30 mA with fibre ends (or other portions) covered by an aluminium foil. A 15-nm-thick Au layer was used for effective masking (inhibiting nanotube growth).

### CALCULATION OF NANOTUBE BRUSH CONTACT AREA

The weight of a sample of  $1 \times 1 \text{ cm}^2$  size and 100  $\mu\text{m}$  height was measured to be 1.7 mg. The weight of a single multiwalled nanotube (outer and inner diameter of 30 and 10 nm, respectively, based on transmission electron microscopy examination, length 100  $\mu\text{m}$ ) is calculated to be  $1.4 \times 10^{-13} \text{ g}$ . Thus the number of nanotubes per unit area is  $1.2 \times 10^8 \text{ mm}^{-2}$ . A three-prong brush as seen in Fig. 1c with 60- $\mu\text{m}$  bristle height and 300- $\mu\text{m}$  span has  $1.7 \times 10^8$  bristles. This number was used to derive the contact area when the brush was placed on a surface or immersed in a solution, assuming all the nanotubes have the same height (length). The surface contact area equals the bristle number multiplied by nanotube tip size, and the liquid contact area equals the bristle number multiplied by individual nanotube surface area.

### MECHANICAL TESTING

Adhesion measurements between nanotube bristles and the fibre handle was done in an Instron 5803 electromechanical tester. The brush handle was fixed by a clamp, and two pieces of gloss-finish multitask tapes (Scotch) were wrapped around the nanotube bristles. During the testing, the Scotch tape grabbed the nanotube bristles and moved away at a constant speed of 1 mm min<sup>-1</sup> until the whole bristle detached from the handle. Three-prong brushes with bristle spans of 1 to 2 mm were used for testing. We observed two stages during the bristle detachment from the brush handle. First, the maximum shear

stress was applied in order to strip nanotube ends off the SiC fibre. The shear strain (5.5%) includes the stretch and tilt of the nanotubes under stress. Second, the whole nanotube bristle moved away along the fibre until complete separation. The shear strain after maximum stress hereby represents the relative displacement between the bristles and the fibre. The remaining stress in this stage ( $\sim 0.05 \text{ MPa}$  at 10%–30% displacement) indicates a small dynamic friction force during nanotube slipping.

### FUNCTIONALIZATION

Functionalization of nanotube brushes with 1,3,6,8-pyrenetetrasulphonic acid tetrasodium salt was carried out by firstly dissolving 200 mg pyrene into 50 ml methanol, and immersing the brushes in the solution for 24 hours at room temperature (with slight stirring to avoid destroying the brush structure). The pyrene-grafted brushes were isolated by filtering the solution through a 200-nm Teflon membrane with complete washing by methanol to get rid of the free pyrene residues, and dried under vacuum at 50 °C for 12 hours. After Ag<sup>+</sup> adsorption, the brushes were placed in a bottle filled with 15% H<sub>2</sub> in Ar for 24 hours to reduce the silver ions into solid particles (Supplementary Information, Fig. S6).

### FOUR-PROBE ELECTRICAL MEASUREMENTS

Four tungsten wires (50  $\mu\text{m}$  in diameter) were fixed in parallel and spaced 2 mm from each other. The brush was placed on the top in contact with the underlying four wires, and its position was adjusted to leave the bristle handle or only the bristle part sitting in between the middle two wires (see insets in Fig. 4a,b). Electrical current was supplied through the outside two wires, and a voltage meter was connected to the two middle wires.

Received 22 March 2005; accepted 5 May 2005; published 12 June 2005.

## References

- www.gordonbrush.com.
- Dresselhaus, M. S., Dresselhaus, G. & Eklund, P. C. *Science of Fullerenes and Carbon Nanotubes* (Academic, San Diego, 1996).
- Baughman, R. H., Zakhidov, A. A. & de Heer, W. A. Carbon nanotubes—the route toward applications. *Science* **297**, 787–792 (2002).
- Poncharal, P., Wang, Z. L., Ugarte, D. & de Heer, W. A. Electrostatic deflections and electromechanical resonances of carbon nanotubes. *Science* **283**, 1513–1516 (1999).
- Frank, S., Poncharal, P., Wang, Z. L. & de Heer, W. A. Carbon nanotube quantum resistors. *Science* **280**, 1744–1746 (1998).
- Yu, M.-F. *et al.* Strength and breaking mechanism of multiwalled carbon nanotubes under tensile load. *Science* **287**, 637–640 (2000).
- Falvo, M. R. *et al.* Bending and buckling of carbon nanotubes under large strain. *Nature* **389**, 582–584 (1997).
- Kim, P., Shi, L., Majumdar, A. & McEuen, P. L. Thermal transport measurements of individual multiwalled nanotubes. *Phys. Rev. Lett.* **87**, 215502 (2001).
- Peigney, A., Laurent, Ch., Flahaut, E., Bacsu, R. R. & Rousset, A. Specific surface area of carbon nanotubes and bundles of carbon nanotubes. *Carbon* **39**, 507–514 (2001).
- Wei, B. *et al.* Organized assembly of carbon nanotubes. *Nature* **495**, 416–417 (2002).
- Andrews, R. *et al.* Continuous production of aligned carbon nanotubes: a step closer to commercial realization. *Chem. Phys. Lett.* **303**, 467–474 (1999).
- Cao, A. *et al.* Direction-selective and length-tunable in-plane growth of carbon nanotubes. *Adv. Mater.* **15**, 1105–1109 (2003).
- Hunt, M. R. C. *et al.* Thermal induced decomposition of single-wall carbon nanotubes adsorbed on H/Si(111). *Appl. Phys. Lett.* **81**, 4847–4849 (2002).
- Zhang, F. & Busnaina, A. Submicron particle removal in post-oxide chemical-mechanical planarization (CMP) cleaning. *Appl. Phys. A* **69**, 437–440 (1999).
- Nanoscience and Nanotechnologies: Opportunities and Uncertainties* www.nanotec.org.uk/finalReport.htm.
- Imahori, H. *et al.* Photoactive three-dimensional monolayers: Porphyrin-alkanethiolate-stabilized gold clusters. *J. Am. Chem. Soc.* **123**, 335–336 (2001).
- Murakami, H., Nomura, T. & Nakashima, N. Noncovalent porphyrin-functionalized single-walled carbon nanotubes in solution and the formation of porphyrin-nanotube nanocomposites. *Chem. Phys. Lett.* **378**, 481–485 (2003).
- Swift, J. A. & Andrews, J. R. Carbon fiber commutator brush for a toner developing device and method for making. US Patent 6289187B1 (2001).
- Wang, X. *et al.* Anisotropic electrical transport properties of aligned carbon nanotube films. *J. Phys. Chem. B* **105**, 9422–9425 (2001).

## Acknowledgements

We thank R. Geier, G. Viswanathan and S. Kar for helpful discussions. This research was supported by the Focus Center New York for Electronic Interconnects and the National Science Foundation Nanoscale Science and Engineering Center for the directed assembly of nanostructures. V. Vedula and M. Nejhad acknowledge the support of ADPICAS project by the Office of Naval Research under the government grant number of N00014-00-1-0692.

Correspondence and requests for materials should be addressed to P. M. A.

Supplementary Information accompanies the paper on www.nature.com/naturematerials.

## Competing financial interests

The authors declare that they have no competing financial interests.